



Widely targeted metabolomic analyses unveil the metabolic variations after stable knock-down of NME4 in esophageal squamous cell carcinoma cells

Shutao Zheng^{1,2} · Tao Liu³ · Qing Liu^{1,2} · Lifei Yang^{1,2} · Qiqi Zhang^{1,2} · Xiujuan Han^{1,2} · Tongxue Shen^{1,2} · Xiao Zhang^{1,2} · Xiaomei Lu^{1,2}

Received: 9 March 2020 / Accepted: 26 May 2020 / Published online: 5 June 2020
© Springer Science+Business Media, LLC, part of Springer Nature 2020

Abstract

NME4, also designated nm23-H4 or NDPK-D, has been known for years for its well-established roles in the synthesis of nucleoside triphosphates, though; little has been known regarding the differential metabolites involved as well as the biological roles NME4 plays in proliferation and invasion of esophageal squamous cell carcinoma (ESCC) cells. To understand the biological roles of NME4 in ESCC cells, lentiviral-based short hairpin RNA interference (shRNA) vectors were constructed and used to stably knock down NME4. Then, the proliferative and invasive variations were assessed using MTT, Colony formation and Transwell assays. To understand the metabolites involved after silencing of NME4 in ESCC cells, widely targeted metabolomic screening was taken. It was discovered that silencing of NME4 can profoundly suppress the proliferation and invasion in ESCC cells in vitro. Metabolically, a total of 11 differential metabolites were screened. KEGG analyses revealed that Tryptophan, Riboflavin, Purine, Nicotinate, lysine degradation, and Linoleic acid metabolism were also involved in addition to the well-established nucleotides metabolism. Some of these differential metabolites, say, 2-Picolinic Acid, Nicotinic Acid and Pipecolinic Acid were suggested to be associated with tumor immunomodulation. The data we described here support the idea that metabolisms occurred in mitochondrial was closely related to tumor immunity.

Keywords NME4 · Invasion · ESCC · Widely targeted metabolomics · Metabolism

Introduction

Nucleoside diphosphate kinases (NDPK) are nucleotide metabolism enzymes encoded by NME, also termed NM23 genes [1]. So far, as many as 10 genes have been identified

to be part of the NDPK/NME family [2]. Among the NME genes, NME4 has been little described and defined in cancers, not to mention in ESCC, with the exception of only one recent study [3] performed surrounding NME4 in non-small cell lung cancer; which stands in stark contrast to the NME1, NME2 or NME3, the paralogs of NME4 in NME gene family, which have been extensively investigated in cancers [4, 5]. On the other hand, although the well-established roles of NME4 in nucleotide metabolism [6] have been known for many years, the metabolites mediated by NME4 in cancer cells remain far less understood. In the present study, we seek to understand the biological roles played by NME4 in ESCC cells and to work out the differential metabolites mediated by NME4, with the aid of widely targeted metabolomics.

In our study, it was discovered that silencing of NME4 was shown to slow the proliferation and invasion of ESCC cells in vitro, indicative of the tumor-promoting roles in ESCC cells. With the help of widely targeted metabolomic screening, a total of 11 differential metabolites were

Electronic supplementary material The online version of this article (<https://doi.org/10.1007/s11010-020-03768-w>) contains supplementary material, which is available to authorized users.

✉ Xiaomei Lu
luxiaomei88@163.com

¹ Clinical Medical Research Institute, First Affiliated Hospital of Xinjiang Medical University, Xinjiang Uygur Autonomous Region, Ürümqi, People's Republic of China

² State Key Laboratory of Pathogenesis, Prevention, Treatment of Central Asian High Incidence Diseases, Xinjiang Uygur Autonomous Region, Ürümqi, People's Republic of China

³ Health Management Center, Xinjiang Medical University, Xinjiang Uygur Autonomous Region, Ürümqi, People's Republic of China

identified, specifically, with 7 being upregulated and 4 downregulated. These differential metabolites identified comprise Inosine, Hypoxanthine-9- β -D-Arabinofuranoside, 15-oxoETE [15-oxo-5Z,8Z,11Z,13E-eicosatetraenoic acid], 2-Picolinic Acid, B-Nicotinamide Mononucleotide, Nicotinic Acid, 6-Methylnicotinamide, Lumichrome, Pantothenol, Pipecolinic Acid and 12,13-EpOME [(\pm)12(13) epoxy-9Z-octadecenoic acid]. Some of these metabolites, for example, 2-Picolinic Acid, Nicotinic Acid and Pipecolinic Acid were suggested to be associated with tumor immunomodulation. Our data shown here firstly defined the oncogenic trait of NME4 in ESCC cells, and our data support the notion that metabolisms occurred in mitochondrial was related to tumor immunity.

Materials and methods

Cell culture and lentivirus-mediated shRNA transfection

ESCC cell lines TE-1, Eca109 and EC9706 cell lines were commercially from Wuhan University (Wuhan, China). All cells were cultured by RPMI 1640 medium (Beijing Solarbio Science and Technology Co., Ltd, Beijing, China) containing 10% fetal bovine serum (Gibco, Carlsbad, CA, USA) and 100 U/mL penicillin and 100 μ g/mL streptomycin at 37 °C in humidified 5% CO₂ incubator. Lentiviruses carrying green fluorescent protein along with scrambled (shRNA-control), or shRNA-NME4 (shRNA-NME4) were purchased from Shanghai GenePharma Co. Ltd. (Shanghai, China). For infection, TE-1 and EC9706 cells were incubated with lentiviruses [multiplicity of infection (MOI) of 15] using polybrene (5 μ g/mL) and enhanced infection solution following the manufacturer's protocol. After 72 h, all fluorescent cells were sorted via flow cytometry. The sorted cells were treated with hygromycin (800 μ g/mL). The shRNA-NME4 target sequence was 5'-CCGGCATGATTGGACACACCGACT CCTCGAGGAGTCGGTGTGTCCAATCATGTTTTT-3'.

RNA extraction and qRT-PCR assay

Total RNA were extracted from ESCC cells with Trizol (Invitrogen, Carlsbad, CA, USA), followed by reverse transcription into cDNA using the PrimeScript RT reagent Kit (Catalog Number RR047A; TaKaRa, Dalian, China) following the manufacturer's protocol. cDNA was amplified and was detected by an ABI 7500 fast system (Applied Biosystems, CA, USA). GAPDH was used as internal control for NME4 relative expression. The primer sequences used were as follows: GAPDH, F-5'-GGAGCGAGATCCCTC CAAAAT-3'; R-5'-GGCTGTTGTCATACTTCTCATGG-3'; NME4, F: 5'-CAACTACCTCCGTCAGCAAGAACC-3'; R:

5'-GTTGGTGGCTCAAACCTCCTCTGG-3'. 2^{- $\Delta\Delta$ c_t} method was taken to calculate the relative expression of NME4. The annealing temperature was set at 55 °C throughout. The qRT-PCR reactions were performed with ABI 7500 real-time PCR system (Applied Biosystems, Foster City, CA, USA).

Western-blot

Total proteins were extracted with Radio-Immunoprecipitation Assay (RIPA) lysis buffer (CWbiotech, Beijing, China) containing the protease inhibitor cocktails (Catalog Number 4693116001; cOmplete; Roche, Switzerland), and the concentration was determined by BCA kit (Solarbio, Beijing, China). The proteins were separated by running 12% SDS-PAGE gel and transblotted to PVDF membranes. Then, membranes were blocked with 5% skimmed milk for 2 h and incubated with the primary antibody anti-NME4 (1:1000; Catalog Number GTX121931, GeneTex, CA, USA), anti-GAPDH (1:1000; Catalog Number TA-08; ZSGB-BIO, Beijing, China) overnight at 4 °C and with secondary antibodies (horseradish-conjugated goat anti-rabbit) for 2 h. The bands were visualized using GelDox XR System (Bio-Rad, CA, USA). Quantity One software (Bio-Rad, CA, USA) was used to quantify the variation of band grey.

MTT

TE-1 and EC9706 cells were seeded at a density of 4 \times 10³/well in a 96-well plate and incubated overnight. At 0, 24, 48, 72, and 96 h, 20 μ L (5 g/L) of MTT (3-[4, 5-dimethyl-2-thiazolyl]-2, 5-diphenyl-2-H-tetrazolium bromide) was added to the designated wells. After a 4 h incubation, the MTT formazan precipitate was dissolved in dimethylsulfoxide (DMSO, 150 μ L/well, Sigma-Aldrich, St. Louis, MO, USA) in a shaker before reading the absorbance at 490 nm using a 96-well plate reader (Bio-Rad, Winooski, VT, USA).

Colony formation assay

For colony formation assay, cells were seeded evenly in 6-well plates (4 \times 10² cells/well) and continuously cultured for 14 days. Then the cells were fixed with methanol for 10 min, stained with 1% crystal violet staining solution for 10 min.

Transwell assay

The invasion assays were performed using a 24-well Transwell chamber with a polycarbonate membrane with a pore size of 8 μ m (Corning, NY, USA). The membrane was coated with 60 μ L of a 1:5 mixture of matrigel (BD Sciences, San Jose, CA, USA) and serum-free RPMI 1640 medium to

form a matrix barrier. After the matrigel was allowed to solidify at 37 °C for 2 h, TE-1 and EC9706 (1×10^5 cells/mL) were added to the upper chamber without serum; the lower chamber was filled with 0.6 mL of medium with 10% FBS. After incubation at 37 °C for 24 h, invaded cells were then rinsed with PBS and stained with crystal violet. The cells remaining at the top of the polycarbonate membrane were removed using cotton swab. The cell numbers in four random fields were manually counted under magnification of 200-fold.

Apoptosis assay

The apoptosis assay was performed with flow cytometry using the Annexin V-FITC Apoptosis Detection Kit (BD Biosciences, San Jose, CA, USA) following the manufacturer's instruction. In brief, Cells were washed twice with cold PBS and resuspended in 400 mL with $1 \times$ binding buffer at a concentration of 1×10^6 cells/mL. Cells were then mixed with 5 mL of the Annexin V-FITC solution and 2 mL of propidium iodide, followed by incubation for 15 min at 4 °C in the dark, finally have these cells analyzed by flow cytometry.

Cell lysate sample

Cell lysate samples from TE-1 and EC9706 cell lines were thawed on ice, then added 1 mL pre-cooled extractants (70% methanol aqueous solution), and whirl for 1 min. Freeze the mixture for 3 min in liquid nitrogen after remove ice for 3 min, it will be whirled for 2 min, circulate this at 3 times. Centrifuge the mixture again with 12,000 r/min at 4 °C for 10 min. Finally take the supernatant into the sample bottle for LC–MS/MS analysis.

HPLC conditions

The sample extracts were analyzed using an LC–ESI–MS/MS system (UPLC, Shim-pack UFLC Shimadzu CBM A system, <https://www.shimadzu.com/>; MS, QTRAP® System, <https://sciex.com/>). The analytical conditions were as follows, UPLC: column, Waters Acquity UPLC HSS T3 C₁₈ (1.8 μm, 2.1 mm * 100 mm); column temperature, 40 °C; flow rate, 0.4 mL/min; injection volume, 2 μL; solvent system, water (0.04% acetic acid): acetonitrile (0.04% acetic acid); gradient program, 95:5 V/V at 0 min, 5:95 V/V at 11.0 min, 5:95 V/V at 12.0 min, 95:5 V/V at 12.1 min, 95:5 V/V at 14.0 min.

ESI–QTRAP–MS/MS

LIT and triple quadrupole (QQQ) scans were acquired on a triple quadrupole-linear ion trap mass spectrometer (QTRAP), QTRAP® LC–MS/MS System, equipped with

an ESI Turbo Ion-Spray interface, operating in positive and negative ion mode and controlled by Analyst 1.6.3 software (Sciex). The ESI source operation parameters were as follows: source temperature 500 °C; ion spray voltage (IS) 5500 V (positive), –4500 V (negative); ion source gas I (GSI), gas II (GSII), curtain gas (CUR) were set at 55, 60, and 25.0 psi, respectively; the collision gas (CAD) was high. Instrument tuning and mass calibration were performed with 10 and 100 μmol/L polypropylene glycol solutions in QQQ and LIT modes, respectively. A specific set of MRM transitions were monitored for each period according to the metabolites eluted within this period.

Statistical analysis

All experiments were carried out independently three times, unless otherwise stated. GraphPad Prism 8.0 software (GraphPad Software, Inc., La Jolla, CA, USA) was used to generate the plots presented and to statistically analyze the difference. The data were expressed as mean \pm standard deviation. A two-tailed, unpaired Student's *T*-test was used for statistical analysis. Two-tailed, unpaired *T*-test with Welch's correction was used to analyze the difference between two groups. Metabolite data were log₂-transformed for statistical analysis to improve normality and normalized. To classify the differential metabolites screened, the 346 metabolites data have been used for cluster analysis by R (www.r-project.org/). The color scale indicates the intensity of the metabolites (log₂-transformed). Unsupervised principal content analysis was conducted by SPSS (Version 18.0, SPSS, Inc., Chicago, IL, USA). Differences in the metabolites between NME4 stably knock-down and control were determined using Welch's *T*-test ($P < 0.01$). Difference was considered to be statistically significant when $P < 0.05$.

Results

NME4 promotes proliferation and invasion of ESCC cells in vitro

To start with, baseline expression of endogenous NME4 was detected on transcriptional level using qRT-PCR technique in the three different ESCC cell lines we enrolled in our experimental setting. In terms of basal NME4 mRNA expression, TE-1 and EC9706 whose NME4 were shown to be remarkably higher than that of ECa109 cell line (Fig. 1a). Therefore, TE-1 and EC9706 were picked up in the experiment that follows. To understand the biological roles NME4 mediates in the growth and motility of ESCC cells, lentiviral-based shRNA vectors targeting against NME4 were constructed and transfected into TE-1 and EC9706 cells, respectively. Knock-down efficiency was evaluated using

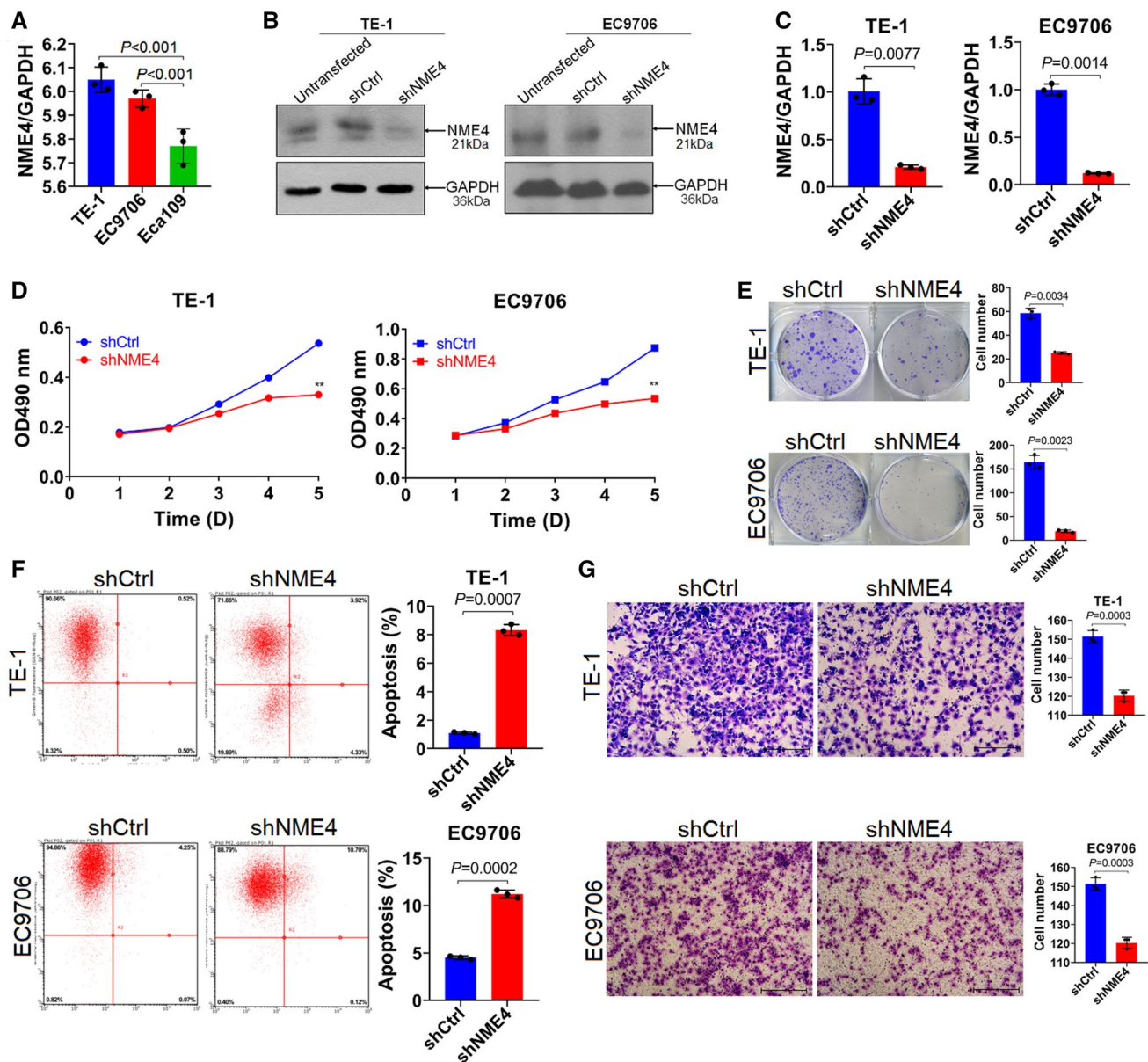


Fig. 1 NME4 promoting proliferation and invasion in ESCC cell lines TE-1 and EC9706. **a** Baseline expression of endogenous NME4 on mRNA level, as detected by qRT-PCR technique, in three different kinds of ESCC cell lines we enrolled in our setting. GAPDH, internal loading control; one-way ANOVA (Bonferroni) was taken to analyze the difference among the three groups. **b** Silencing effect, as determined by western-blot, of ESCC cell lines TE-1 and EC9706 transfected with lentiviral-based shRNA-NME4 and its corresponding control, respectively. A total of 50 μ g proteins were loaded, the relative variation of NME4 was normalized to GAPDH, acted as internal loading control, **c** quantitative analysis of variation of NME4 expression shown in western-blot. Two-tailed, unpaired *T*-test with Welch's correction was used ($T=10.30$, $df=2.112$, P value=0.0077; $T=25.59$, $df=2.031$, P value=0.0014), and **d** proliferative varia-

tions, as assayed by MTT method, after NME4 was stably silenced in TE-1 and EC9706 cells. Of note, the error bars on the graphs were too small to be seen here. $**P<0.001$ compared with control using the independent sample *T*-test. **e** In parallel with MTT assays, proliferative variations, as determined by colony formation assay, after inhibition of NME4. The exact *P* scores labeled were calculated using two-tailed, unpaired *T*-test with Welch's correction. **f** Likewise, apoptotic variations were analyzed using flow cytometry in TE-1 and EC9706 cells whose NME4 were stably knocked down. The exact *P* values labeled were calculated using two-tailed, unpaired *T*-test with Welch's correction. **g** Invasive variations were assessed using Transwell assays in TE-1 and EC9706 cells whose NME4 were silenced. The exact *P* values labeled were calculated using two-tailed, unpaired *T*-test with Welch's correction

western-blot after sorting of cells. It was exhibited that NME4 were significantly silenced in TE-1 and EC9706 cells (Fig. 1b, c). Based on the interferential effect displayed,

the roles of NME4 mediate in proliferation and invasion were appraised by MTT, colony formation and Transwell assays. It was exhibited that, compared with control group,

proliferative abilities of ESCC cells were markedly slowed down after NME4 were stably knocked down (Fig. 1d); which were corroborated by colony formation assay undertaken in parallel (Fig. 1e). Meanwhile, the apoptotic assay revealed that apoptotic rates were dramatically increased in ESCC cells whose NME4 were silenced in comparison with control (Fig. 1f). Transwell assay showed that invasive capabilities of ESCC cells were seriously suppressed relative to control (Fig. 1g). Together, all the data we presented above explicitly indicate that NME4 can promote the proliferation and invasion of ESCC cells.

Differential metabolic products screened out after NME4 were stably knocked down

Having understood the oncogenic traits of NME4 in ESCC cells, we next attempted to explore the involvement of NME4 in metabolism of cell lines derived from ESCC that has not been clear yet. To profile the differential metabolites of ESCC cells after TE-1 and EC9706 cells whose endogenous NME4 were stably silenced, widely targeted metabolomic screening strategy was taken (Supplementary Fig. 1). Expectantly, a great deal of differential metabolites, up to 346 kinds of metabolic products (Supplementary Table 1), were obtained. In spite of these numerous differential metabolites that were eventually screened, it turned out that there were only 11 metabolites that were significantly differential between experimental group and control, with 7 metabolites being upregulated and 4 downregulated (Table 1), after cluster analyses performed (Fig. 2a, b). To further comb out these metabolites that were significantly differential, KEGG (Kyoto Encyclopedia of Genes and Genomes) analyses were carried out. KEGG analyses showed that, NME4 were mainly predicative to be involved in metabolic pathways (Fig. 2c). Specifically, the 11 differential metabolites identified comprise Inosine, Hypoxanthine-9- β -D-Arabinofuranoside, 15-oxoETE

[15-oxo-5Z,8Z,11Z,13E-eicosatetraenoic acid], 2-Picolinic Acid, B-Nicotinamide Mononucleotide, Nicotinic Acid, 6-Methylnicotinamide, Lumichrome, Pantothenol, Pipecolinic Acid and 12,13-EpOME [(\pm)12(13)epoxy-9Z-octadecenoic acid] (Fig. 3). These metabolites, if biochemically classified, fundamentally belong to the nucleotide metabolism (Inosine, Hypoxanthine-9- β -D-Arabinofuranoside and B-Nicotinamide Mononucleotide), followed by CoOthers-Enzyme Factor and vitamin (Nicotinic Acid and Pantothenol), then came the Oxidized lipid (15-oxoETE and 12, 13-EpOME) and other metabolism in terms of quantity (Table 1).

Discussion

In the current investigation, the oncogenic trait of NME4 was firstly defined in vitro in cell lines derived from ESCC in our experimental setting, displaying that NME4 was able to promote the proliferation and invasion of ESCC cells. Metabolically, NME4 was found to be chiefly implicated in the metabolic signaling pathway, outside of nucleotide metabolism. To our knowledge, this is the first report defining the oncogenic traits of NME4 and profiling the differential metabolites after NME4 was stably silenced in ESCC cells.

NME4, also called NM23D, NM23H4, Nm23-H4, or NDPK-D, belongs to the group I members of NME family [7] that can be divided in two groups in mammals according to phylogenetic analyses [8]. Group I comprised NME1, NME2, NME3 and NME4, which share from 58 to 88% identity and are all catalytically active, as systematically reviewed by Lacombe et al. [7]. Unlike the NME1 [9], NME2 [10] or NME3 [11] that have been extensively studied in cancers from different tissues and organs, by contrast, only few data have been available regarding NME4 in human cancers. The original report mentioning Nm23-H4 in cancer came from neuroblastoma [12]

Table 1 Differential metabolites that were significant after stable knock-down of NME4 in ESCC cells

Index	Compounds	Class	Fold change	log ₂ FC	Type
MEDN164	Inosine	Nucleotide metabolomics	2.90219	1.53714	Up
MEDN444	Hypoxanthine-9- β -D-Arabinofuranoside	Nucleotide metabolomics	2.75054	1.45972	Up
MEDN771	15-oxoETE [15-oxo-5Z,8Z,11Z,13E-eicosatetraenoic acid]	Oxidized lipid	2.78114	1.47567	Up
MEDP116	2-Picolinic Acid	Pyridine and pyridine derivatives	4.49532	2.16842	Up
MEDP180	B-Nicotinamide Mononucleotide	Nucleotide metabolomics	2.88966	1.5309	Up
MEDP246	Nicotinic Acid	CoOthersEnzyme Factor and vitamin	4.15246	2.05397	Up
MEDP821	6-Methylnicotinamide	Pyridine and pyridine derivatives	2.44907	1.29223	Up
MEDP890	Lumichrome	Others	0.4661	-1.1013	Down
MEDP249	Pantothenol	CoOthersEnzyme Factor and vitamin	0.39707	-1.3325	Down
MEDP358	Pipicolinic Acid	Organic acid and its derivatives	0.09187	-3.4442	Down
MEDN767	12,13-EpOME [(\pm)12(13)epoxy-9Z-octadecenoic acid]	Oxidized lipid	0.4575	-1.1282	Down

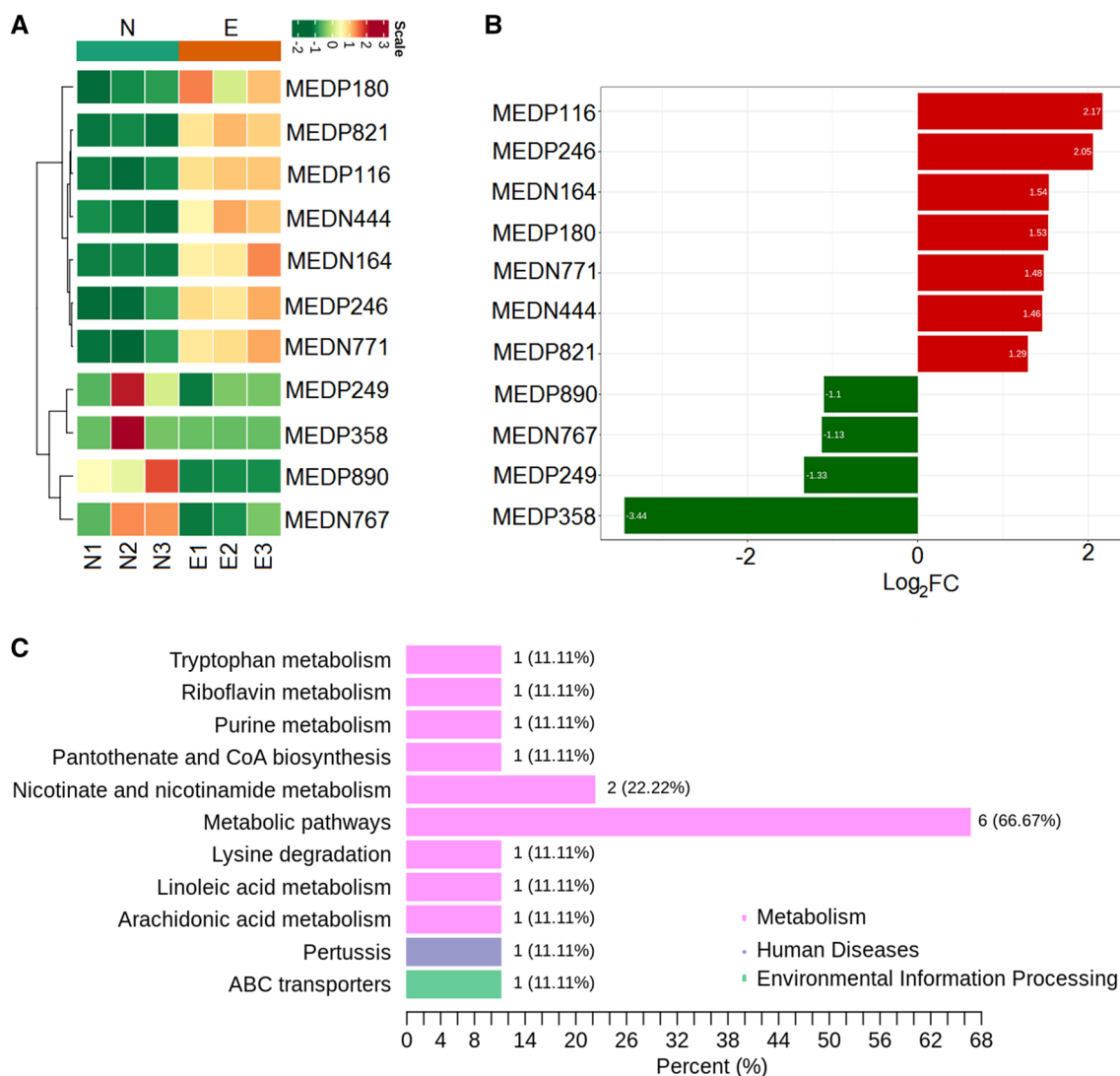


Fig. 2 Cluster and KEGG analyses of the differential metabolites identified after stable silencing of NME4 in ESCC cells. **a** Cluster analyses, as shown in the form of heat map, of the differential metabolites that were significant after downregulation of NME4 in ESCC cells. In heat map we presented here, on which the products indexed from top to bottom denote MEDP116, 2-Picolinic Acid; MEDN444, Hypoxanthine-9- β -D-Arabinofuranoside; MEDN164, Inosine; MEDP246, Nicotinic Acid; MEDN771, 15-oxoETE [15-oxo-5Z,8Z,11Z,13E-eicosatetraenoic acid]; MEDP249, Pantothenol;

MEDP358, Pipecolinic Acid; MEDP890, Lumichrome; MEDN767, 12,13-EpOME [(\pm)12(13)epoxy-9Z-octadecenoic acid], **b** bar chart of fold change of metabolic products, indexed totally the same as those in heat map and **c** Kyoto Encyclopedia of Genes and Genomes (KEGG) analysis of differentially metabolic products. Y-axis represents the metabolic signaling pathways that were possibly involved; X-axis denotes the ratio of the number of the metabolic products obtained to the total number of metabolic products annotated in the signaling pathway

where Nm23-H4 was just incidentally mentioned, without much attention being paid. Almost at the same time, in another study concerning diffuse astrocytoma [13], in which Nm23-H4 was also acknowledged in the differential cDNAs that were screened. Later on, in another study about colorectal and renal carcinoma [14], Nm23-H4 was shown to be over-expressed on mRNA level; giving a cue that Nm23-H4 might be oncogenic in colorectal and renal cancer. One subsequent study performed on protein level in human gastric and colon cancer [15], congruently

supported that Nm23-H4 protein was over-expressed in neoplastic tissues compared with normal control, suggesting that Nm23-H4 may be involved in the oncogenesis of gastric and colon cancer. Despite these implicit suggestions from earlier studies, no explicit causal relationship between NME4 or Nm23-H4 and carcinogenesis has been established until the very recent study [3] appeared. In the study [3], lentivirus-mediated knock-down of NME4 was reported to be able to inhibit the abilities of proliferation and colony formation, suggestive of the tumor-promoting

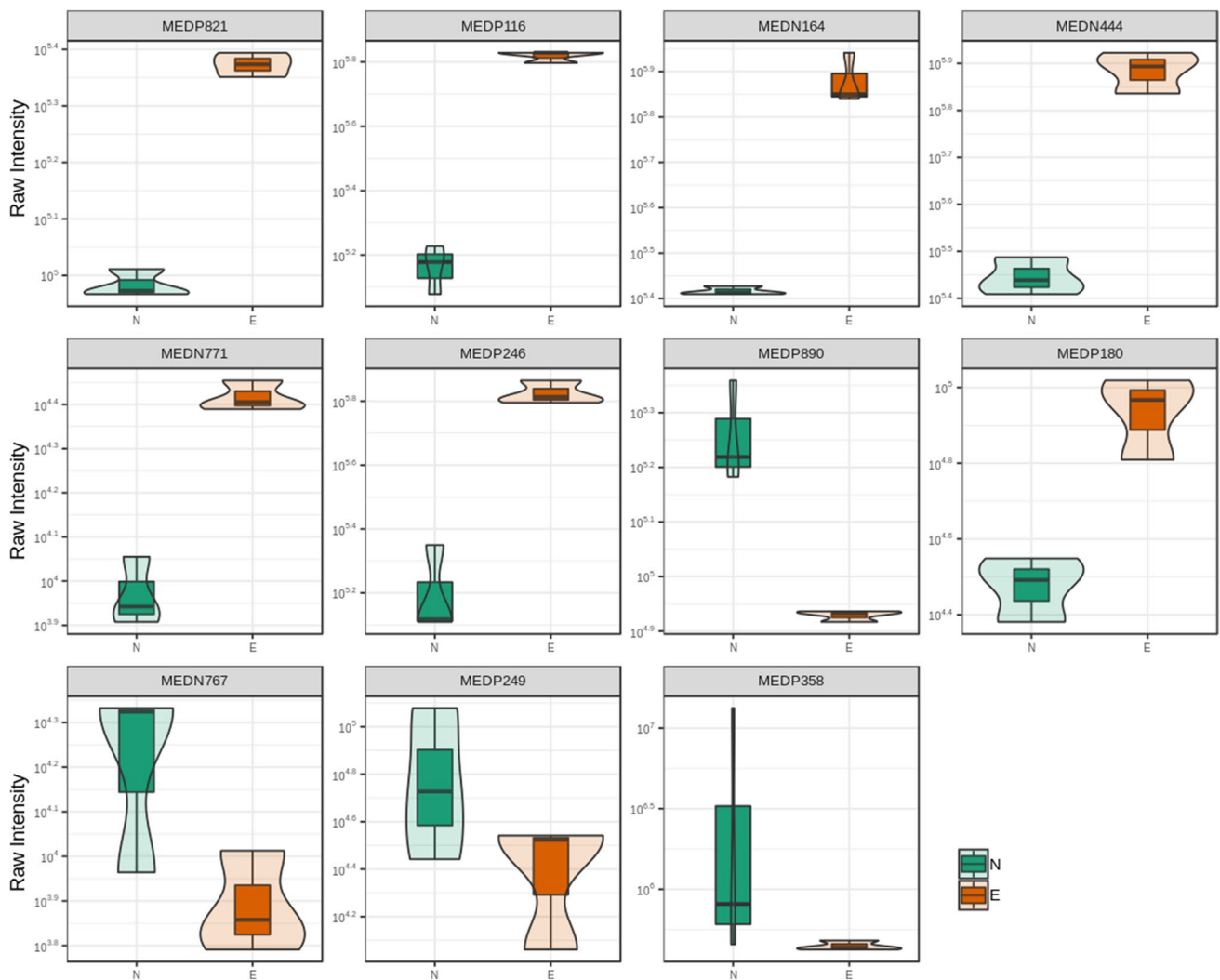


Fig. 3 Violin plots of metabolic products we screened out that were significantly differential between control group (denoted as N) and experimental group (represented by E). The differential metabolic products indexed MEDP821, 6-Methylnicotinamide; MEDP116, 2-Picolinic Acid; MEDN164, Inosine; MEDN444, Hypoxanthine-9- β -D-Arabinofuranoside; MEDN771, 15-oxoETE [15-oxo-

5Z,8Z,11Z,13E-eicosatetraenoic acid]; MEDP246, Nicotinic Acid; MEDP890, Lumichrome; MEDP180, B-Nicotinamide Mononucleotide; MEDN767, 12,13-EpOME [(±)12(13)epoxy-9Z-octadecenoic acid]; MEDP249, Pantothenol; MEDP358, Pipecolinic Acid, respectively

role in non-small cell lung cancer; which was in agreement with our observation described here.

Although available evidence acknowledged NME4 as a key player in bioenergetics and lipid signaling and an important contributor to the quality control of the mitochondria (reviewed in [7]), little has been known regarding the differential metabolites mediated by NME4 in cancer cells. Given this, attempt has been made using the widely targeted metabolomic screening to work out the differential metabolites in ESCC cells whose NME4 were stably knocked down compared with control, showing that there were 11 metabolites identified that were significantly differential between silencing of NME4 and control group. Notably, 2-picolinic acid and nicotinic acid whose absolute folds were shown to

be far greater than others among the differential metabolites, totaling seven, that were identified to be upregulated. Having identified these differential metabolites, we reasoned that NME4 could negatively regulate these metabolites identified to be upregulated in our setting, which warrants further investigation and confirmation in clinical samples. Biochemically, 2-picolinic acid identified here was a pyridine derivative that involved in kynurenine pathway of tryptophan metabolism [16]. Albeit the role of 2-picolinic acid in ESCC cells was unclear, recent evidence emerged suggesting that picolinic acid has much bearing on immune modulation in cancers [16, 17]. The role picolinic acid mediates in the modulation of tumor immunity within ESCC remains elusive that needs to be further investigated. Nicotinic acid, also

called vitamin PP or nicotinamide, much like 2-picolinic acid, biochemically, was implicated in the kynurenine pathway that is the principal route of L-tryptophan catabolism eventually giving birth to the picolinic acid and nicotinamide [18]. Despite the nicotinic acid has been known for decades, its immunomodulatory role in ESCC remains obscure that needs to be further studied.

Among the four metabolites identified to be downregulated with the knock-down of NME4 in ESCC cells, pipecolinic acid has to be mentioned and discussed here because of its most conspicuous downregulation. In pathophysiological environment, little has been described concerning pipecolinic acid. By contrast, the role of pipecolinic acid in immunity has been uncovered gradually with recent works surrounding pipecolinic acid in immunomodulation, which mainly focused on plant, rarely on human. In a more recent study [19], pipecolinic acid was mechanistically found to confer systemic immunity by regulating free radicals in plant. This observation inevitably leads to a speculation that pipecolinic acid may, as in plant, work in the similar way in human cancers. Future investigations on pipecolinic acid in tumor immunity are required to address the speculation.

NME4 mainly located in mitochondria where NME4 have been proposed to work to synthesize ATP or nucleoside diphosphate (NTP) for protein and nucleic acid synthesis [20]. Among its related pathways implicated was nucleotides metabolism, which was expectantly confirmed by our KEGG analyses revealing that Tryptophan, Riboflavin, Purine, Nicotinate, lysine degradation, and Linoleic acid metabolism were also involved in addition to the well-established nucleotides metabolism. The observation we made here was reminiscent of one recent review underscoring that Tryptophan metabolism was associated with cancer immunomodulation [21], therefore can be used as a potential therapeutic target in cancers. Our study presented here back up the current view [22, 23] hold that metabolism, particularly occurred in mitochondria, was associated with tumor immunity. Despite these, there were still two limitations inherent in our study described here. For one thing, all the conclusions drawn on the basis of two kinds of ESCC cell lines in vitro, should have been extended to clinical samples; secondly, differential metabolites identified in our setting warrants further confirmation using the different ESCC cell lines with larger sample size.

In conclusion, NME4 was shown to promote the proliferation and invasion of ESCC cells in vitro. Metabolically, with the aid of widely targeted metabolomic screening, differential metabolites, totaling 11, were identified including Inosine, Hypoxanthine-9- β -D-Arabinofuranoside, 15-oxoETE [15-oxo-5Z,8Z,11Z,13E-eicosatetraenoic acid], 2-Picolinic Acid, B-Nicotinamide Mononucleotide, Nicotinic Acid, 6-Methylnicotinamide, Lumichrome, Pantothenol, Pipecolinic Acid and 12,13-EpOME [(\pm)12(13)

epoxy-9Z-octadecenoic acid]. Some of these metabolites were suggested to be associated with tumor immunomodulation. Our data described above support the relationship between metabolisms occurred in mitochondrial and tumor immunity.

Acknowledgements The study was partly supported by Nature Science Foundation of China (NSFC.81960552, 81960527, 81960527, U1603284, 81860511), and partly by Science and Technology Projects of Xinjiang Uygur Autonomous Region (2018E02067), by Tian-shan Xuesong Project of the Xinjiang Uygur Autonomous Region (2018XS19).

Compliance with ethical standards

Conflict of interest The authors declare that there was no conflict of interests.

References

- Boissan M, Schlattner U, Lacombe ML (2018) The NDPK/NME superfamily: state of the art. *Lab Invest* 98:164–174. <https://doi.org/10.1038/labinvest.2017.137>
- Boissan M, Dabernat S, Peuchant E, Schlattner U, Lascu I, Lacombe ML (2009) The mammalian Nm23/NDPK family: from metastasis control to cilia movement. *Mol Cell Biochem* 329:51–62. <https://doi.org/10.1007/s11010-009-0120-7>
- Wang W, Dong M, Cui J, Xu F, Yan C, Ma C, Yi TW, Dong J, Wei Y (2019) NME4 may enhance nonsmall cell lung cancer progression by overcoming cell cycle arrest and promoting cellular proliferation. *Mol Med Rep* 20:1629–1636. <https://doi.org/10.3892/mmr.2019.10413>
- Liu L, Li M, Zhang C, Zhang J, Li G, Zhang Z, He X, Fan M (2018) Prognostic value and clinicopathologic significance of nm23 in various cancers: a systematic review and meta-analysis. *Int J Surg* 60:257–265. <https://doi.org/10.1016/j.ijssu.2018.10.035>
- Wang QH, Han W, Chen MB, Bao J, Wang BF (2018) Prognostic value of NM23 in patients with gastric cancer: a systematic review and meta-analysis. *J Cancer Res Ther* 14:S556–S564. <https://doi.org/10.4103/0973-1482.183188>
- Milon L, Rousseau-Merck MF, Munier A, Erent M, Lascu I, Capeau J, Lacombe ML (1997) nm23-H4, a new member of the family of human nm23/nucleoside diphosphate kinase genes localised on chromosome 16p13. *Hum Genet* 99:550–557. <https://doi.org/10.1007/s004390050405>
- Lacombe ML, Tokarska-Schlattner M, Boissan M, Schlattner U (2018) The mitochondrial nucleoside diphosphate kinase (NDPK-D/NME4), a moonlighting protein for cell homeostasis. *Lab Invest* 98:582–588. <https://doi.org/10.1038/s41374-017-0004-5>
- Lacombe ML, Milon L, Munier A, Mehus JG, Lambeth DO (2000) The human Nm23/nucleoside diphosphate kinases. *J Bioenerg Biomembr* 32:247–258. <https://doi.org/10.1023/a:1005584929050>
- Han W, Shi CT, Cao FY, Cao F, Chen MB, Lu RZ, Wang HB, Yu M, He DW, Wang QH, Wang JF, Xu XX, Ding HZ (2016) Prognostic value of NME1 (NM23-H1) in patients with digestive system neoplasms: a systematic review and meta-analysis. *PLoS ONE* 11:e0160547. <https://doi.org/10.1371/journal.pone.0160547>
- Thakur RK, Yadav VK, Kumar P, Chowdhury S (2011) Mechanisms of non-metastatic 2 (NME2)-mediated control of metastasis across tumor types. *Naunyn Schmiedebergs Arch Pharmacol* 384:397–406. <https://doi.org/10.1007/s00210-011-0631-0>

11. Yang T, Chen BZ, Li DF, Wang HM, Lin XS, Wei HF, Zeng YM (2016) Reduced NM23 protein level correlates with worse clinicopathologic features in colorectal cancers: a meta-analysis of pooled data. *Medicine (Baltim)* 95:e2589. <https://doi.org/10.1097/MD.0000000000002589>
12. Negroni A, Venturelli D, Tanno B, Amendola R, Ransac S, Cesi V, Calabretta B, Raschella G (2000) Neuroblastoma specific effects of DR-nm23 and its mutant forms on differentiation and apoptosis. *Cell Death Differ* 7:843–850. <https://doi.org/10.1038/sj.cdd.4400720>
13. Huang H, Colella S, Kurrer M, Yonekawa Y, Kleihues P, Ohgaki H (2000) Gene expression profiling of low-grade diffuse astrocytomas by cDNA arrays. *Cancer Res* 60:6868–6874
14. Hayer J, Engel M, Seifert M, Seitz G, Welter C (2001) Over-expression of nm23-H4 RNA in colorectal and renal tumours. *Anticancer Res* 21:2821–2825
15. Seifert M, Welter C, Mehraein Y, Seitz G (2005) Expression of the nm23 homologues nm23-H4, nm23-H6, and nm23-H7 in human gastric and colon cancer. *J Pathol* 205:623–632. <https://doi.org/10.1002/path.1724>
16. Heng B, Lim CK, Lovejoy DB, Bessede A, Gluch L, Guillemin GJ (2016) Understanding the role of the kynurenine pathway in human breast cancer immunobiology. *Oncotarget* 7:6506–6520. <https://doi.org/10.18632/oncotarget.6467>
17. Kimura Y, Negishi H, Matsuda A, Endo N, Hangai S, Inoue A, Nishio J, Taniguchi T, Yanai H (2018) Novel chemical compound SINCRO with dual function in STING-type I interferon and tumor cell death pathways. *Cancer Sci* 109:2687–2696. <https://doi.org/10.1111/cas.13726>
18. Adams S, Teo C, McDonald KL, Zinger A, Bustamante S, Lim CK, Sundaram G, Braidy N, Brew BJ, Guillemin GJ (2014) Involvement of the kynurenine pathway in human glioma pathophysiology. *PLoS ONE* 9:e112945. <https://doi.org/10.1371/journal.pone.0112945>
19. Wang C, Liu R, Lim GH, de Lorenzo L, Yu K, Zhang K, Hunt AG, Kachroo A, Kachroo P (2018) Pipecolic acid confers systemic immunity by regulating free radicals. *Sci Adv* 4:eaar4509. <https://doi.org/10.1126/sciadv.aar4509>
20. Gordon DM, Lyver ER, Lesuisse E, Dancis A, Pain D (2006) GTP in the mitochondrial matrix plays a crucial role in organellar iron homeostasis. *Biochem J* 400:163–168. <https://doi.org/10.1042/BJ20060904>
21. Platten M, Nollen EAA, Rohrig UF, Fallarino F, Opitz CA (2019) Tryptophan metabolism as a common therapeutic target in cancer, neurodegeneration and beyond. *Nat Rev Drug Discov* 18:379–401. <https://doi.org/10.1038/s41573-019-0016-5>
22. Mills EL, Kelly B, O'Neill LAJ (2017) Mitochondria are the powerhouses of immunity. *Nat Immunol* 18:488–498. <https://doi.org/10.1038/ni.3704>
23. Sukumar M, Kishton RJ, Restifo NP (2017) Metabolic reprogramming of anti-tumor immunity. *Curr Opin Immunol* 46:14–22. <https://doi.org/10.1016/j.coi.2017.03.011>

Publisher's Note Springer Nature remains neutral with regard to jurisdictional claims in published maps and institutional affiliations.